Biomass Conversion and Biorefinery (2024) 14:7857–7872
https://doi.org/10.1007/s13399-022-02926-y

ORIGINAL ARTICLE

Sorption-enhanced gasification of municipal solid waste for hydrogen production: a comparative techno-economic analysis using limestone, dolomite and doped limestone

Mónica P. S. Santos[1] · **Dawid P. Hanak**[1]

Received: 15 March 2022 / Revised: 3 June 2022 / Accepted: 6 June 2022 / Published online: 23 June 2022
© The Author(s) 2022

Abstract
Sorption-enhanced gasification has been shown as a viable low-carbon alternative to conventional gasification, as it enables simultaneous gasification with in-situ CO_2 capture to enhance the production of H_2. CaO-based sorbents have been a preferred choice due to their low cost and wide availability. This work assessed the technical and economic viability of sorption-enhanced gasification using natural limestone, doped limestone with seawater and dolomite. The techno-economic performance of the sorption-enhanced gasification using different sorbents was compared with that of conventional gasification. Regarding the thermodynamic performance, dolomite presented the worst performance (46.0% of H_2 production efficiency), whereas doped limestone presented the highest H_2 production efficiency (50.0%). The use of dolomite also resulted in the highest levelised cost of hydrogen (5.4 €/kg against 5.0 €/kg when limestone is used as sorbent), which translates into a CO_2 avoided cost ranging between 114.9 €/tCO_2 (natural limestone) and 130.4 €/tCO_2 (dolomite). Although doped limestone has shown a CO_2 avoided cost of 117.7 €/tCO_2, this can be reduced if the production cost of doped limestone is lower than 42.6 €/t. The production costs of new sorbents for CO_2 capture and H_2 production need to be similar to that of natural limestone to become an attractive alternative to natural limestone.

Keywords Sorption-enhanced gasification · Waste-to-fuel · Hydrogen production · Dolomite · Doped limestone

1 Introduction

Global carbon dioxide (CO_2) emissions have been rising for over a century now [1]. Although a significant emission reduction was recorded in 2021, mostly due to reduced economic activity caused by COVID-19, the global energy-related CO_2 emissions bounced back to the pre-pandemic levels in 2021 [2]. Thus, unless the CO_2 and other greenhouse emissions are significantly reduced, the 1.5 °C and 2 °C global warming scenarios will be overcome until the end of this century [3]. Carbon capture and storage (CCS), as well as the reduction of fossil fuel dependency, have been identified as routes to tackle CO_2 emissions. The latter can be achieved by expanding the production of cleaner fuels and energy carriers, including hydrogen.

Hydrogen (H_2) or H_2-rich syngas production has been thoroughly investigated from different types of biomass and wastes feedstocks such as sawdust [4], sewage sludge [5, 6], hazelnut shells [7], wood chips [8], wood pellets [9], palm kernel shell [10], plastics [11], food waste [12] and municipal solid waste (MSW) [13]. Although biomass is a renewable source and accessible at a reduced price, the generalised use of biomass for bioenergy production can start competing with food and crops production. Thus, wastes from agriculture, landfills, food, biomass residues, sewage sludge and manure, are regarded as sustainable feedstocks and should play a role in decarbonisation [14].

Considering the current state of solid waste management, there are significant differences between developed and developing countries, with the latter relying on open waste dumping [15]. Such practice, on top of open burning and unsanitary landfills, raises several environmental issues comprising global warming, ozone and resources

✉ Mónica P. S. Santos
monica.santos@cranfield.ac.uk

✉ Dawid P. Hanak
d.p.hanak@cranfield.ac.uk

[1] Energy and Power, School of Water, Energy and Environment, Cranfield University, Bedford, Bedfordshire MK43 0AL, UK

depletion, damage of ecosystems and human health hazards [16]. Furthermore, it is forecasted that the annual $CO_{2,eq}$ emissions associated with solid wastes can reach 2.6 billion tonnes by 2050 if no improvements in waste management are deployed. It is because the amount of solid waste generated by developing countries is forecasted to triple by that year [15].

A range of technologies for thermochemical conversion of MSW have been considered, including plasma gasification [17, 18], chemical looping combustion [19], gasification [20, 21], gasification integrated with simultaneous chemical and calcium looping [22], and sorption-enhanced gasification (SEG) [13, 23–27]. MSW SEG was assessed by He et al. [23] in a lab-scale fixed bed reactor at the gasification temperature of 900 °C. They have investigated the catalytic effect of calcined dolomite on the gasification performance, as well as the effect of the steam/MSW ratio on the gas composition and H_2 yield. They found that the increase in a steam/MSW ratio increased the H_2 mole fraction and the H_2 yield, which peaked (53% and 43 mol H_2/kg MSW, respectively) for a steam/MSW ratio of 1.04. Hu et al. [24] used CaO as a CO_2 sorbent to study the effect of parameters such as gasification temperature, Ca/C molar ratio and moisture content on the H_2 yield and syngas composition. The experiments were carried out in a lab-scale fixed bed reactor. They found that a maximum H_2 mole fraction in syngas (49.4%) could be achieved at the gasification temperature of 750 °C, a CaO/MSW molar ratio of 0.7 and moisture content in MSW of 40%. Similarly, Zhou et al. [25] selected a fixed bed to study the effect of CaO sorbent on the performance of MSW steam SEG. In that case, a lab-scale batch type reactor was used. The H_2 mole fraction in the syngas has been shown to increase by 15% points with the addition of CaO sorbent, from around 35% when no sorbent was present in the reactor. This result was achieved for a CaO/MSW mass ratio of 1 and at the gasification temperature of 700 °C. They have also shown that CaO acts as a CO_2 sorbent and catalyst, being responsible for enhancing the MSW devolatilization and char gasification. The use of waste marble powder as a CaO-based sorbent and simultaneously a catalyst was investigated by Irfan et al. [13] in a lab-scale batch-type reactor. The performance of MSW SEG, including syngas yield and composition, tar content and carbon conversion efficiency, were evaluated at different gasification temperatures, steam/MSW and sorbent/MSW ratios. They found that the increase in gasification temperature, steam/MSW and sorbent/MSW ratios promoted the H_2 mole fraction in the syngas. Consequently, the syngas yield and the carbon conversion efficiency have increased. However, it is important to notice that an increase in the considered operating conditions also resulted in a decrease in the tar formation. The concept of MSW SEG has also been proven to be a feasible technology for H_2-rich gas production at a 30 kW_{th} bubbling fluidised bed (BFB) plant [26]. This study considered limestone as a CO_2 sorbent, mostly because of its availability and low cost. Yet, this study did not consider the deterioration of the sorbent performance, which is a known challenge of using limestone as a sorbent [28], because the set-up was operated in a semi-batch mode. Finally, Santos et al. [27] have compared the techno-economic performance of MSW steam SEG with that of conventional steam gasification for H_2 production. The authors have shown that MSW SEG could deliver a higher H_2 production efficiency (48.7%) than conventional gasification (47.7%). Yet, such improvement is obtained at the expense of higher H_2 production costs, the levelised cost of H_2 (*LCOH*) increased from 2.1–3.2 €/kg H_2 (conventional gasification) to 4.5–5.1 €/kg H_2 (SEG).

Natural materials such as the shells from mollusc, scallop, oyster and mussel as well as eggshells have been shown viable as a CO_2 sorbent. However, the calcined sorbent also presented deactivation along with the carbonation/calcination cycles [29]. Moreover, it would be challenging to convert such waste to sorbent for large-scale applications. Thus, alternative sorbents for SEG need to be considered. These sorbents, besides the high CO_2 sorption capacity, should also present fast sorption kinetics, good mechanical properties, good cyclic stability and be economically viable [30]. If the properties of synthetic sorbents are easier to be manipulated, the high cost of the chemical precursors results in a higher cost of sorbent production [31].

Therefore, several approaches have been considered to enhance the performance of natural CaO-based sorbents, including the incorporation of inert materials with high Tammann temperatures, doping of sorbent and additional treatments including hydration or chemical pretreatment.

Several inert materials have been studied as potential support materials to improve the sorbent stability, including aluminium oxide (Al_2O_3) [32, 33], magnesium oxide (MgO) [33], zirconium oxide (ZrO_2) [33, 34], titanium oxide (TiO_2) [35], yttrium oxide (Y_2O_3) [33], and silica (SiO_2) [36]. Because these materials modify the sorbent skeleton, the sorbent granulation is improved and the sintering phenomenon is prevented. However, these sorbents are more expensive than natural CaO-based sorbents.

Hydration is another technique investigated in the current literature to increase the sorption capacity of the CaO-based sorbents. Water hydration [37] or steam hydration [38] can be used to improve the CO_2 sorption capacity of the fresh sorbent. This technique has also been applied for reactivation of the spent sorbent [39]. In the latter case, the enhancement of sorption capacity is attributed to the formation of calcium hydroxide ($Ca(OH)_2$). Since the molecule $Ca(OH)_2$ presents a higher molar volume than CaO, this contributes to the formation of cracks and then paths. This morphology alteration increases the surface area and pore volume, enhancing the CO_2 sorption [40].

The chemical treatment is another approach considered in the current literature to improve the CO_2 sorption capacity of the sorbent. In this approach, an enhancement of sorption capacity is achieved by treating the sorbent with chemicals such as acetic acid and pyroligneous acid [30]. Li et al. [41] have found that after 20 cycles of carbonation/calcination, the conversion of limestone pretreated with acetic acid increased by more than a factor of 3 when compared with that of natural limestone (0.5 against 0.15). This can be attributed to the higher surface area and higher pore volume of treated limestone, which prevents the sintering phenomenon.

The CO_2 sorption capacity of sorbent has been shown to be enhanced by doping the CaO-based sorbents with sodium chloride (NaCl) [42], hydrogen bromide (HBr) [43] and seawater [44, 45]. Salvador et al. [42] have studied the effect of doping limestone with $0.5\%_{wt}$ NaCl in a thermogravimetric analyser (TGA) and fluidised bed reactor. While in the tests performed in the fluidised bed reactor, there was no positive effect on the CO_2 sorption capacity. In the TGA experiments, this figure was higher than that for natural limestone after 14 cycles. It should be noted that in the first cycles the natural limestone presented a better performance than the doped one. The addition of $0.167\%_{mol}$ HBr to limestone was studied by González et al. [43] in a fluidised bed reactor. The authors found that the CO_2 sorption capacity of limestone, after 13 cycles, doubled when compared with the natural limestone. Xu et al. [44] have investigated the possibility of using an abundant and cheap material, seawater, as a dopant to improve the CO_2 sorption capacity of limestone. They have carried out 20 cycles of carbonation/calcination in a fixed bed reactor. The authors concluded the CO_2 sorption capacity was maximum for $0.25\%_{wt}$ of dopant. Morona et al. [46] have also studied the doping of limestone with different concentrations of seawater. After the sorbent had undergone 20 cycles of carbonation/calcination, the carbonation conversion was evaluated in a TGA. Unlike the previous work, the authors observed a deleterious effect on sorbent performance when dopped with seawater, which can be associated with an excessive addition of dopant [47]. The use of seawater as a dopant was also studied by González et al. [45], although in this work, the experiments were performed in a fluidised bed reactor. Similarly, to previous work, the authors have investigated different concentrations of dopant. They concluded that the addition of seawater to the four limestones tested improved the sorbent performance.

Similar to limestone, dolomite is another inexpensive natural CaO-based sorbent available worldwide. De La Calle Martos et al. [48] have compared the limestone and dolomite CO_2 capture performance in a TGA, undergoing 20 cycles of carbonation/calcination. They concluded that dolomite compared with limestone presented the following advantages: lower regeneration temperature, lower deactivation along with the cycles, superior CaO conversion, and thus, a higher CO_2 capture capacity. Although dolomite and doped limestone have been extensively assessed, the mentioned studies were carried out from a CO_2 capture performance standpoint of view. Moreover, the majority of studies that assessed SEG to date have solely focused on syngas production through MSW gasification with in-situ CO_2 capture, disregarding the sorbent regeneration step that is essential for the continuous operation of the SEG process. Santos and Hanak [27] have reported for the first time the techno-economic feasibility of a cyclic SEG of MSW for H_2 production. However, that study only assessed the H_2 production costs for SEG of MSW using natural limestone as sorbent and, therefore, no comparative study has been carried out for other sorbents. Martínez et al. [26] and Santos and Hanak [27] have shown that SEG using limestone is a feasible technology to convert waste-to-fuel, despite the fact that the economic assessment performed by Santos and Hanak [27] has shown it is still not competitive. Yet, dolomite and doped limestone may be an attractive alternative to natural limestone sorbent, promoting the deployment of SEG of MSW. Dolomite presents higher CO_2 desorption kinetics, which implies lower calcination temperature and, thus, a lower energy penalty. Doped limestone has shown to have a lower reactivity decaying over the cycles, improving CO_2 sorption capacity and, therefore, leading to an enhancement of H_2 production. Thus, it is crucial to evaluate these alternative sorbents for H_2 production with in-situ CO_2 capture.

This work aims to examine whether alternative sorbents can improve the techno-economic viability of MSW SEG for H_2 production. The techno-economic assessment of the MSW SEG was performed for three different CaO-based sorbents, including natural limestone, doped limestone with seawater and dolomite. Furthermore, an assessment of the MSW SEG design specifications and economic assumptions on the process energy, economic and environmental performance was assessed via a sensitivity analysis.

2 Process and model description

MSW, whose characteristics are shown in Table 1, was selected as feedstock for hydrogen production through SEG. The MSW SEG process is presented in the simplified block flow diagram in Fig. 1. The operating conditions are listed in Table 2. The MSW processing rate was assumed to be 500 t of MSW per day, corresponding to approximately 100 MW_{th}. The SEG process model, based on a set of mass and energy balances, was developed in Aspen Plus. The model was based on the Gibbs free energy minimisation approach. The physical properties of the components were assessed using the Peng-Robinson equation of state with Boston-Mathias modifications. To simplify the model, it was considered that:

Table 1 Municipal solid waste properties [52]

Proximate analysis [$\%_{wt}$ db]	
Ash	7.12
Fixed carbon	15.36
Volatile matter	77.52
Ultimate analysis [%wt db]	
Carbon	49.51
Oxygen	35.69
Hydrogen	6.42
Nitrogen	0.78
Sulphur	0.48
Moisture [$\%_{wt}$]	9.34
LHV [MJ/kg]	19.99

db dry basis, *LHV* lower heating value

(1) the process is isothermal, (2) the process operates under steady-state conditions, (3) the heat losses and the pressure drops are negligible, (4) graphitic carbon is the only compound of char, (5) ash is inert and (6) the formation of tar and higher hydrocarbon is negligible. The SEG process was validated with the experimental data reported by Fremaux et al. [49] and Armbrust et al. [50]. The syngas composition was obtained at 700 °C, 800 °C and 900 °C for a range of *SBR* between 0.5 and 1.0, besides the H_2 yield obtained at the same temperatures and for the *SBR* 0.5, 0.7 and 1.0 were compared with that obtained by the model. The experiments carried out by Armbrust et al. [50] at two different syngas compositions were used to validate the carbonation reaction and thus the H_2-rich gas composition. Besides the syngas composition, the carbonation temperature (637 °C and 643 °C) and sorbent looping ratio (7.0 and 8.6) were used to validate the process. The SEG process validation is described in detail by Santos and Hanak [27].

Since the raw MSW is not suitable for gasification, this is subjected to a pretreatment [51]. In the first stage, the recyclables and non-recyclables are separated (primary separation). In the second stage, mechanical treatment is carried out to produce briquettes suitable to be gasified. Therefore, the energy requirement and the costs of pretreatment have been accounted for in the techno-economic evaluation. The data detailed by Luz et al. [51] was used to appraise both.

As shown in Fig. 1, the MSW SEG plant comprises a gasifier operating in parallel with a calciner. In this work, three CaO precursor sorbents were selected, natural limestone, dolomite and doped limestone with seawater. In the SEG process, sorbent acts as a heat and CO_2 carrier, and circulates between the two interconnected fluidised beds. The CO_2 removal by the sorbent takes place in a gasifier (Eq. (1)), whereas the sorbent regeneration, represented by Eqs. (2) and (3), takes place in a calciner. It should be noted that Eq. (3) corresponds to the first stage of dolomite decomposition, which occurs at around 700 °C and is not dependent on the CO_2 content in the gas phase present in the calciner [48].

Carbonation:

$$\begin{aligned} &\mathrm{CaO(s)} + \mathrm{CO_2(g)} \rightarrow \mathrm{CaCO_3(s)} \\ &\Delta H = -178\ \mathrm{kJ/mol} \end{aligned} \tag{1}$$

Calcination:

$$\begin{aligned} &\mathrm{CaCO_3(s)} \rightarrow \mathrm{CaO(s)} + \mathrm{CO_2(g)} \\ &\Delta H = 178\ \mathrm{kJ/mol} \end{aligned} \tag{2}$$

Dolomite decomposition:

$$\begin{aligned} &\mathrm{MgCa(CO_3)_2(s)} \rightarrow \mathrm{CaCO_3(s)} + \mathrm{MgO(s)} + \mathrm{CO_2(g)} \\ &\Delta H = 127\ \mathrm{kJ/mol} \end{aligned} \tag{3}$$

To compensate for the sorbent deactivation and corresponding decrease in the CaO conversion, a fresh stream of sorbent, called make-up (F_0), is fed to the calciner. Equation (4) represents the maximum average conversion (X_{ave}) that can be accomplished by the sorbent over the cycles of carbonation/calcination and is based on the model presented by Rodríguez et al. [28]. The maximum average conversion depends on the properties of sorbent (a_1, a_2, f_1, f_2 and b), the carbonated (f_{carb}) and calcined sorbent fraction (f_{calc}), the fresh make-up sorbent rate (F_0) and the sorbent circulation rate (F_R). The sorbent properties were determined by the curve-fitting procedure. The experimental data detailed by Zhen-Shan et al. [53] and González et al. [45] were used to determine the sorbent characteristics for dolomite and doped limestone, respectively. It is noteworthy that since the gasification and CO_2 capture take place in the gasifier, the solid stream leaving the gasifier comprises the sorbent and the ash. Part of the ash is purged with the deactivated sorbent after the calcination.

$$X_{ave} = (F_0 + F_R r_0) f_{calc} \left[\frac{a_1 f_1^2}{F_0 + F_R f_{carb} f_{calc}(1 - f_1)} + \frac{a_2 f_2^2}{F_0 + F_R f_{carb} f_{calc}(1 - f_2)} + \frac{b}{F_0} \right] \tag{4}$$

The heat required by the endothermic calcination reaction is met by the oxy-combustion of the unconverted char and a fraction of the tail gas from the H_2 upgrading unit. It was assumed that the O_2 is delivered by a cryogenic air separation unit (ASU), which corresponds to energy consumption of 200 $kW_{el}h/tO_2$ [54]. Since the gasification and CO_2 capture take place simultaneously in the same reactor, the equilibrium of water gas shift reaction, Eq. (5), is altered and the forward reaction is favoured, enhancing the H_2 formation. Moreover, this kind of integration is beneficial because the heat released by the exothermic carbonation reaction and the sensible heat of sorbent sustains the endothermic gasification process.

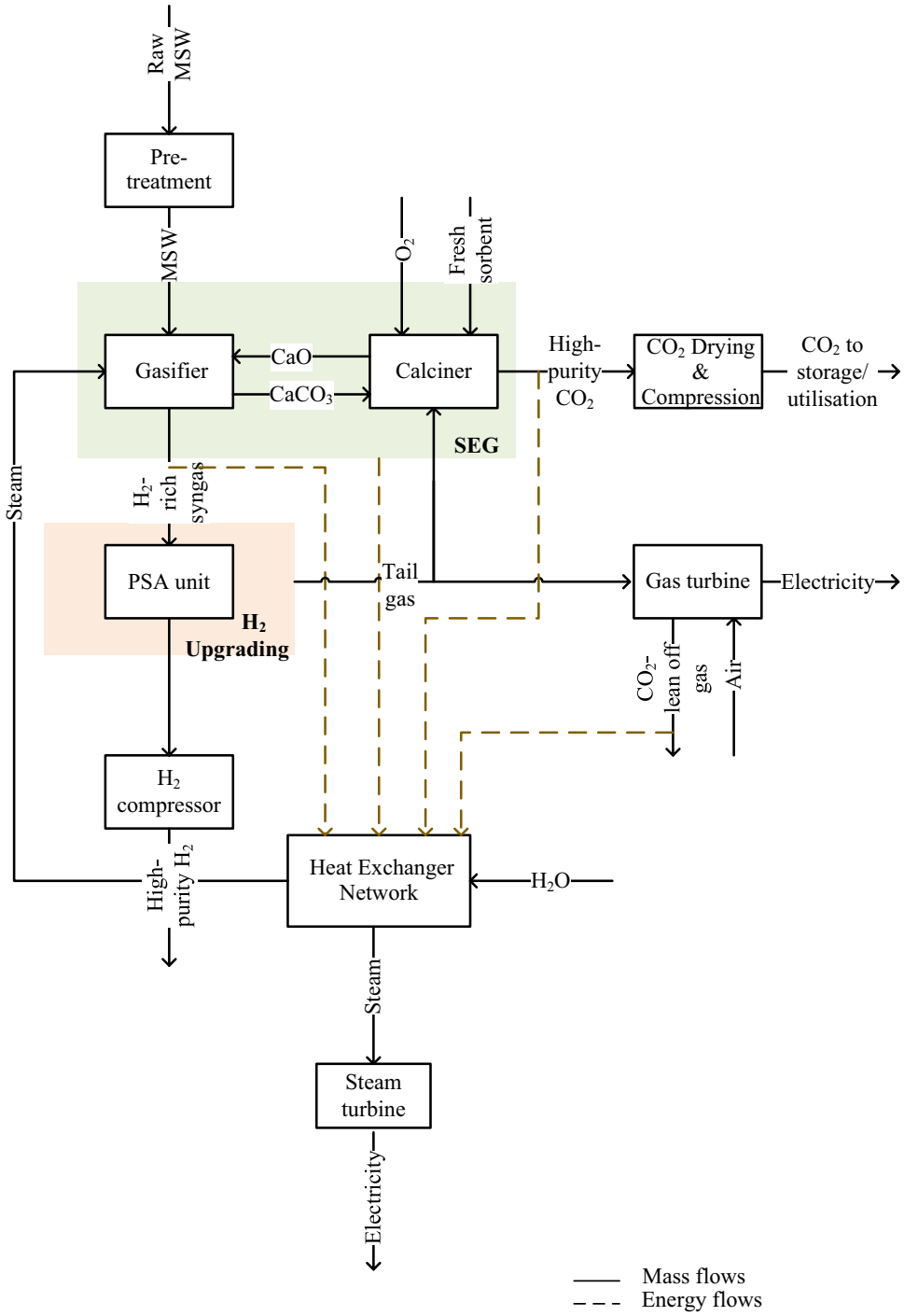

Fig. 1 Simplified block diagram representation of sorption-enhanced gasification of municipal solid waste for hydrogen production

Water gas shift:

$$\mathrm{CO(g) + H_2O(g) \leftrightarrow CO_2(g) + H_2(g)} \qquad \Delta H = \pm 40.9\ \mathrm{kJ/mol} \tag{5}$$

Two reactors, Gibbs reactor and stoichiometric reactor, were used to represent the gasification and carbonation processes, respectively. As these processes occur in the same reactor, a heat stream is connected between the Gibbs and stoichiometric reactors. A Gibbs reactor was also used to model the calcination process. It should be noted that besides the reactor units of SEG, a pressure swing adsorption (PSA) unit, an ASU, a gas turbine, a heat exchanger network and a CO_2 compression unit are also components of the plant. Because the temperature of flue gas leaving the combustor chamber is close to the adiabatic flame temperature, this is mixed with compressed air at 20 bar to lower the turbine inlet temperature to 1268 °C. Then, the flue gas is

Table 2 Summary of the key sorption-enhanced gasification model assumptions

Unit operation	Parameter	Value
Sorption-enhanced gasification		
Sorption-enhanced gasifier	Temperature (°C)	650
	Steam-to-biomass ratio (wt/wt)	0.5–1.7 (dolomite)
		0.5–2.0 (limestone and doped limestone)
	Carbonation extent (-)	0.7
	CO_2 capture efficiency in carbonator (%)	90.0
Calciner	Temperature (°C)	850 (dolomite)
		900 (limestone and doped limestone)
	Calcination extent (-)	0.95
	Excess oxygen ($\%_{vol,dry}$)	2.5
	Ratio between fresh make-up sorbent rate and sorbent circulation rate (-)	0.02
H_2-rich syngas upgrading		
Compression		
Compressor	Polytropic efficiency (%)	80.0
	Mechanical efficiency (%)	99.6
H_2-rich syngas final stream	Temperature (°C)	30
	Pressure (bar)	34
PSA	H_2 recovery (%)	93.0
	H_2 purity ($\%_{vol}$)	99.9
	Temperature (°C)	30
	Feed pressure (bar)	34
	Tail gas pressure (bar)	1
	Delivery pressure (bar)	60
CO_2 compression		
Compressors	Polytropic efficiency (%)	80.0
	Mechanical efficiency (%)	99.6
Pump	Isentropic efficiency (%)	80.0
	Mechanical efficiency (%)	99.6
CO_2 final stream	Temperature (°C)	25.0
	Pressure (bar)	110.0
Steam cycle		
Condenser	Fresh water temperature (°C)	10.0
Low-pressure turbine	Isentropic efficiency (%)	88
	Mechanical efficiency (%)	98
Intermediate-pressure turbine	Isentropic efficiency (%)	94
	Mechanical efficiency (%)	99.8
High-pressure turbine	Isentropic efficiency (%)	92.0
	Mechanical efficiency (%)	99.8
Live steam	Temperature (°C)	593.0
	Pressure (bar)	154.0
Gas turbine		
	Turbine inlet temperature (°C)	1268
	Turbine isentropic efficiency (%)	80
	Turbine mechanical efficiency (%)	99.6
	Compressor outlet pressure (bar)	20
	Combustor pressure drop (%)	2
Fresh material [59]	Dolomite ($57.5\%_{wt}$ $CaCO_3$, $42.44\%_{wt}$ $MgCO_3$, $0.01\%_{wt}$ SiO_2, $0.02\%_{wt}$ Fe_2O_3, $0.03\%_{wt}$ Al_2O_3)	
	Limestone ($95.0\%_{wt}$ $CaCO_3$, $3.5\%_{wt}$ $MgCO_3$, $0.6\%_{wt}$ SiO_2, $0.4\%_{wt}$ Fe_2O_3, $0.5\%_{wt}$ Al_2O_3)	

expanded in the turbine that is coupled with the generator to produce electricity. It was assumed that the H_2-rich stream produced in the sorption-enhanced gasifier is upgraded in a PSA unit, which was modelled as a black box. According to Luberti et al. [55] and Hu [56], an H_2 stream with 99.9% of purity and 93% of recovery rate is achievable at 34 bar. Consequently, the H_2-rich syngas produced in the sorption-enhanced gasifier is compressed from 1 bar to 34 bar in a 9-stage compressor. It should be noted the H_2-rich stream upgrading is preceded by cooling the gas to 30 °C and water removal stages. The heat recovered during these stages is integrated into the heat exchanger network to produce steam that is used as the gasifying agent in the SEG process. Then, the high-purity H_2 stream is subjected to compression until 60 bar. Part of the tail gas from the PSA unit is used to meet the calciner energy requirement and the remaining part is burnt in the gas turbine to generate electricity. In the CO_2 compression unit, the pressure of the high-purity CO_2 stream produced in the calciner is increased to 110 bar and the temperature is reduced to 25 °C [57]. The high-grade heat of the high-purity CO_2 stream, along with the one from the CO_2-lean off-gas, is recovered in the heat exchanger network and used in the steam cycle to produce electricity. The SEG model, as well as the steam cycle, have been described in detail and validated elsewhere [27, 58].

3 Techno-economic feasibility assessment

In this work, the techno-economic analysis of MSW SEG for dolomite and doped limestone was evaluated at its best performance to ensure a fair comparison. As explained in Sect. 4.1, it was assumed that the best performance of each sorbent is achieved for the highest value of *SBR* at which the plant is energy self-sufficient. These figures were benchmarked with that obtained for SEG using limestone as sorbent and conventional gasification [27].

3.1 Thermodynamic performance indicators

H_2 production efficiency, gross power efficiency, net power efficiency and total efficiency were the indicators chosen to appraise and compare the thermodynamic performance of SEG and conventional gasification. The H_2 production efficiency, described by Eq. (6), is the coefficient between the heat content of the product, H_2 and the fuel heat content, MSW. LHV_{H_2} and $\dot{m}_{H_2}$ represent the lower heating value and mass flow rate of H_2, respectively, and LHV_{MSW} and $\dot{m}_{MSW}$ correspond to the same variables for MSW.

$$\eta_{H_2} = \frac{\dot{m}_{H_2} \bullet \mathrm{LHV}_{H_2}}{\dot{m}_{MSW} \bullet \mathrm{LHV}_{MSW}} \tag{6}$$

The ratio between the sum of electric power output from the gas turbine and the steam cycle ($W_{el,gross}$) and the fuel heat content, MSW, defines the gross power efficiency ($\eta_{el,gross}$) defined by Eq. (7).

$$\eta_{el,gross} = \frac{W_{el,gross}}{\dot{m}_{MSW} \bullet \mathrm{LHV}_{MSW}} \tag{7}$$

Equation (8) represents the net power efficiency ($W_{el,net}$) that is defined as the ratio between the net electric power output ($W_{el,net}$) and the fuel heat content, MSW. The former is the difference between the gross electric power output and the electric power demand by the auxiliary equipment.

$$\eta_{el,net} = \frac{W_{el,net}}{\dot{m}_{MSW} \bullet \mathrm{LHV}_{MSW}} \tag{8}$$

The sum of H_2 production and net power efficiencies, defines the total efficiency (η_{tot}) represented by Eq. (9).

$$\eta_{tot} = \frac{\left(\dot{m}_{H_2} \bullet \mathrm{LHV}_{H_2}\right) + W_{el,net}}{\dot{m}_{MSW} \bullet \mathrm{LHV}_{MSW}} \tag{9}$$

3.2 Economic performance indicators

The *LCOH* and the cost of CO_2 avoided (*AC*) were selected as indicators to assess the economic performance of SEG. These were used to benchmark the performance of MSW SEG with that of conventional gasification. The *LCOH*, minimum H_2 selling price at which the profits offset the total costs over the project lifetime, was estimated based on the net present value (*NPV*). The capital costs of each piece of equipment were scaled up using a scaling size factor. All the correlations are listed as supplementary information. The approach used to assess the total capital requirement is detailed in Santos and Hanak [27]. Although the inflation was not considered over the project lifetime, the capital costs were updated to the year 2017 using Chemical Engineering Plant Cost Index (CEPCI) [60].

Since in this work all the costs are presented in Euro (€), if the costs reported in the literature were in a different currency, an average conversion rate for the year 2017 was used [61]. The average conversion rate for the year 2017 and the other economic parameters and assumptions are summarised in Table 3. The operating and maintenance costs account for the variable and the fixed costs. The former was calculated based on the production output, including the costs associated with raw materials, utilities and CO_2 transport and storage. To estimate the latter, it was assumed 17.8% of the total capital requirement is spent to cover the costs associated with salaries,

Table 3 Parameters used to assess the economic performance

Parameter	Value
Unit cost of electricity exported to the grid (€/$MW_{el}h$) [62]	40.0
Limestone unit cost (€/t) [8]	11.6
Dolomite unit cost (€/t)	11.6
Doped limestone unit cost (€/t)	58.0[a]
Fresh water unit cost (€/m^3) [8]	2.4
CO_2 transport and storage cost (€/t) [63]	20.0
Others	
Project interest rate (%) [64, 65]	8.8
Project lifetime (y) [64, 65]	25.0
Capacity factor (%) [64, 65]	80.0
Average GBP/EUR exchange rate 2017 [61]	1.1418
Average USD/EUR exchange rate 2017 [61]	0.8898
CO_2 emission allowance price (€/tCO_2) [66]	39.6
Gate fee (€/t_{MSW}) [67]	40.0

[a]The price of doped limestone was assumed to be 5 times the price of natural limestone (11.6 €/t) to account the doping and drying of sorbent

insurance and tax payments, mortgage payments and indirect expenses of running a business [8].

The cost of CO_2 avoided, given by Eq. (10), is the ratio between the difference of *LCOH* and the difference of equivalent CO_2 emissions $e_{CO_2,eq}$ of conventional gasification and of sorption-enhanced gasification plants. The equivalent CO_2 emission accounts for the direct and indirect CO_2 emissions. The latter is associated with the electric power imported or exported by the plant. The subscripts Gasf and SEG refer to conventional gasification and sorption-enhanced gasification, respectively.

$$AC = \frac{LCOH_{SEG} - LCOH_{Gasf}}{e_{CO_2,eq,Gasf} - e_{CO_2,eq,SEG}} \quad (10)$$

4 Results and discussion

The techno-economic performance of SEG using dolomite and doped limestone with seawater as sorbent was assessed based on the indicators defined in the previous section. These sorbents' performance was compared with that obtained for SEG using natural limestone. The SEG performance was benchmarked with the conventional gasification.

4.1 Thermodynamic performance

A parametric study was carried out varying the steam-to-biomass ratio (*SBR*) between 0.5 and 1.7 and between 0.5

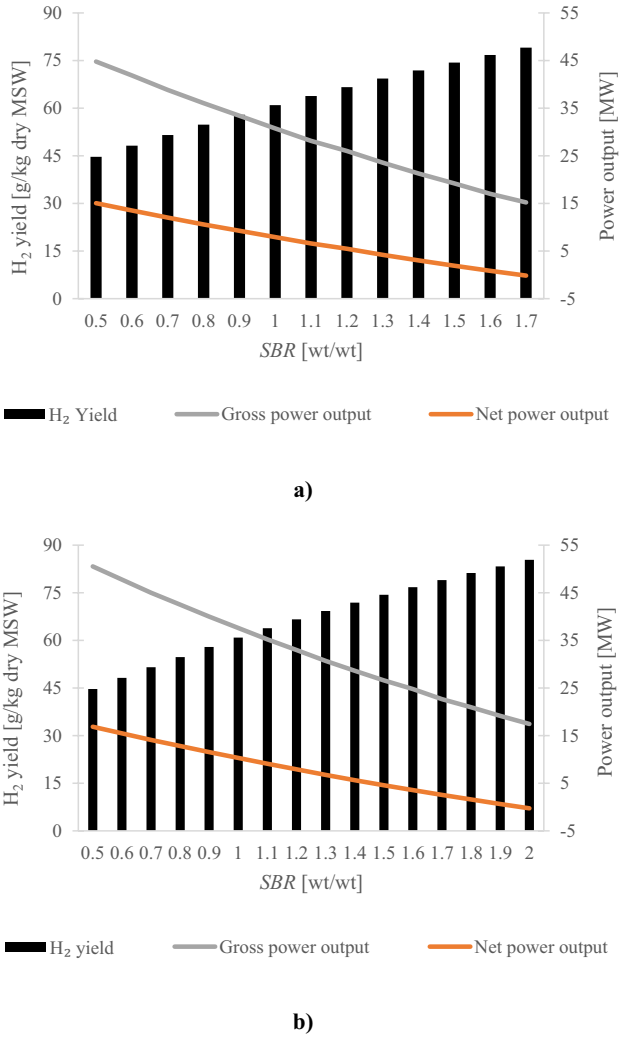

Fig. 2 Effect of steam-to-biomass ratio, at gasification temperature of 650 °C, on hydrogen yield, gross and power outputs for sorption-enhanced gasification using (**a**) dolomite and (**b**) doped limestone with seawater as sorbent

and 2.0 for SEG using dolomite and doped limestone, respectively. The *SBR* ranges are different because it was assumed that the plant is energetic self-sufficient, which after the last point of the interval (*SBR* = 1.7 and *SBR* = 2.0, for dolomite and doped limestone, respectively) is no more valid. The gasification temperature was kept constant at 650 °C because for temperatures behind 680 °C the CO_2 capture is controlled by the equilibrium of carbonation reaction [26]. The effect of *SBR* on the H_2 yield and gross and net power outputs is shown in Fig. 2. This analysis revealed a trade-off between H_2 production and the net power output. It can be seen the profiles of the analysed variables are similar for both sorbents. The H_2 yield increased gradually with the *SBR* increase, which is due to the equilibrium shift of steam-methane reforming and water gas shift reactions. As the H_2O content increases, the equilibrium changes and the forward

reaction is favoured, thus boosting the H_2 production. On the other hand, the gross and net power outputs decreased which can be attributed to the higher power consumption for the H_2 final product compression and CO_2 compression, as well as higher energy consumption for steam production. Moreover, the power generation by the gas turbine and the steam cycle was penalised. This is due to the reduced availability of the tail gas, from the H_2 upgrading unit, to be burnt in the gas turbine and the heat excess to be recovered. These trends were observed for both sorbents with some particularities. In the case of dolomite, the lower electric power generated by the gas turbine was compensated by the higher electric power generated by the steam cycle. It was because there was less tail gas available to be burnt in the gas turbine and there was more heat excess recovered in the steam cycle. The latter can be attributed to the fact that more solids were recirculated. Therefore, more heat was released at the carbonator, which is in agreement with the study carried out by Ortiz et al. [68] for CaL process. In the case of doped limestone, since less tail gas was needed to meet the energy requirement of the calciner, the electric power generated by the gas turbine compensated the lower one generated by the steam cycle.

The effect of *SBR* on the thermodynamic performance indicators, described in Sect. 3, is presented in Fig. 3. As would be expected, the H_2 production, gross power and net power efficiencies follow the trends seen for H_2 yield, gross and net power outputs (Fig. 2). The total efficiency increased marginally in the *SBR* range investigated. Because this work intends to compare the H_2 production from MSW SEG using different sorbents, to perform a fair comparison, the optimum *SBR* was determined as the value at which there was a change from positive to negative sign on the net power output. This means the plant is self-sufficient from an energy standpoint and the H_2 production is maximised. Thus, the optimum *SBR* was 1.6 and 1.9 for dolomite and doped limestone, respectively. For higher SBR values, the electricity generated by the system was insufficient to meet the auxiliary power requirement of the SEG Process. Consequently, the SEG plant would need to draw electricity from the grid. At the optimum *SBR*, the SEG process was found to result in an H_2 yield of 76.7 and 83.3 g/kg dry MSW (Fig. 2) for dolomite and doped limestone, respectively. This translated into an H_2 production efficiency of 46.0% and 50.0% (Fig. 3). Similar to the H_2 production efficiency, the use of dolomite resulted in a lower total efficiency by 4 percentage points, 46.8% (dolomite) compared to that of the SEG process using doped limestone (50.6%). Although the calciner temperature can be reduced from 900 to 850 °C when dolomite was used as sorbent, a higher sorbent make-up was fed to the calciner due to the presence of inert material. This result is in agreement with the reported for the CaL process [68]. Consequently, more tail gas from the H_2 upgrading unit

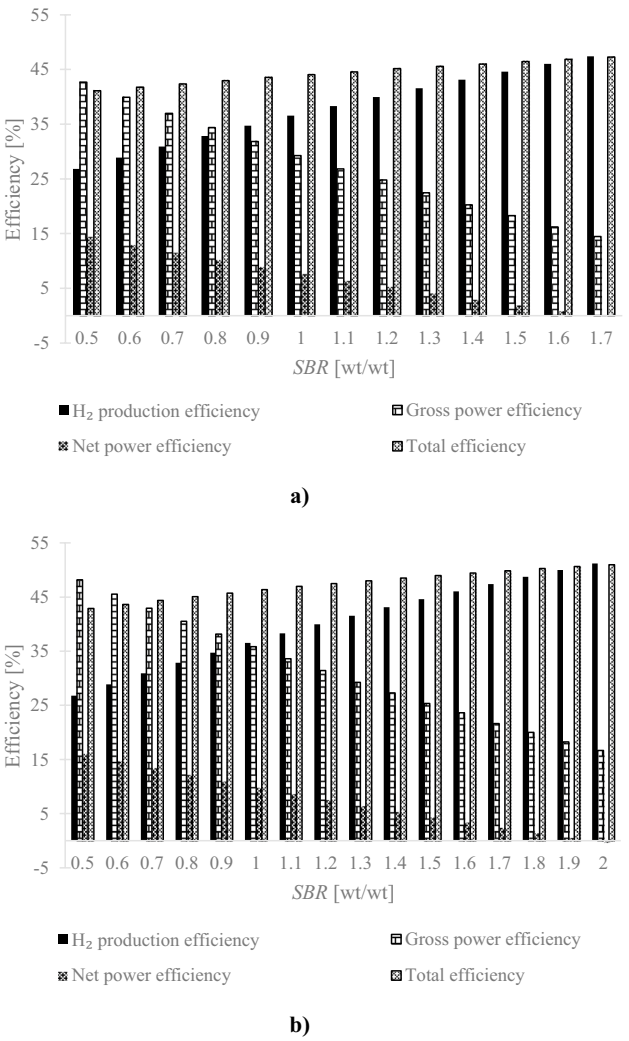

Fig. 3 Effect of steam-to-biomass ratio, at gasification temperature of 650 °C, on hydrogen production, gross power, net power and total efficiencies for sorption-enhanced gasification using (**a**) dolomite and (**b**) doped limestone with seawater as sorbent

was consumed as fuel in the calciner and less was available for power generation in the gas turbine. Besides, more power was required by the ASU and the CO_2 compression unit. The latter can be explained by the fact that more fresh material was calcined. At the carbonator operating conditions (650 °C), the MgO content in the dolomite is not carbonated and more fresh sorbent is needed. Therefore, the SEG process using dolomite has shown to have the highest heat requirement in the calciner (4.9 GJ/tCO_2); on the other hand, the SEG process using doped limestone presents the lowest figure (4.6 GJ/tCO_2).

4.2 Economic performance

Because there is still some discrepancy between the economic data reported in the literature, the economic

assessment was performed for different scenarios. In scenario 1, considered as the baseline scenario, there was no gate fee or fossil CO_2 emissions tax considered; scenario 2 accounted for a gate fee but no tax on fossil CO_2 emissions; in scenario 3, the levy of fossil CO_2 emissions but without a gate fee was considered; and in scenario 4, the application of both, gate fee and fossil CO_2 emissions tax, were considered.

In the techno-economic evaluation of scenario 2 and scenario 4, it was assumed that the SEG plant charges a fee of 40.0 €/t_{MSW}, gate fee, to the waste disposers [67]. In scenario 3 and scenario 4, to estimate the fossil CO_2 emissions, it was assumed there were no fluctuations in MSW composition over the year and 60% of the carbon present was of fossil origin [67]. It is worth noting that the CO_2 emissions from fresh sorbent calcination were also accounted for in the calculation of fossil CO_2 emissions [58]. These CO_2 emissions are the only ones levied with the CO_2 emission allowance price (EUA), which was estimated taking into account the average value for the first trimester of 2021, 39.6 €/tCO_2 [66]. This is a conservative figure since the value in the current year of 2022 is close to 90.0 €/tCO_2.

The estimated *LCOH* and CO_2 avoided cost of SEG using dolomite and doped limestone for each scenario are depicted in Figs. 4 and 5, respectively. The *LCOH* of SEG is also compared with conventional gasification in Fig. 4. It can be seen from this figure that there is no difference in the trend observed for each sorbent over the scenarios. For both sorbents, the selection of SEG technology over gasification technology led to an increase in the *LCOH*. However, this rise ranged between 79.5 and 100.0% in the case of dolomite and for doped limestone felt between 67.9 and 89.2%. This can be attributed to the higher conversion in the carbonator

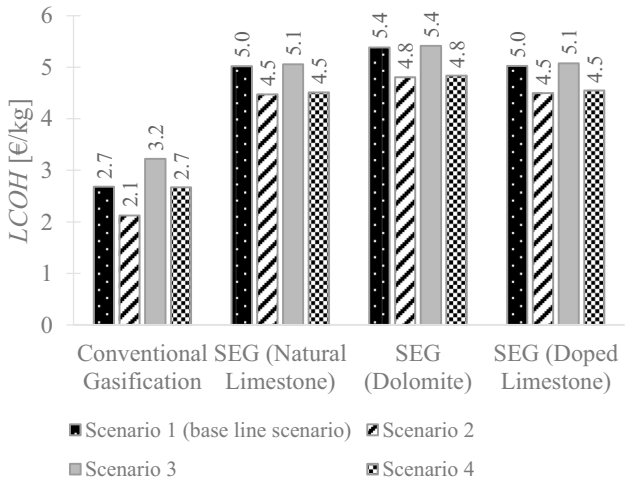

Fig. 4 Comparison of levelised cost of hydrogen of conventional gasification and of sorption-enhanced gasification using natural limestone, dolomite and doped limestone with seawater as sorbent, for the different scenarios

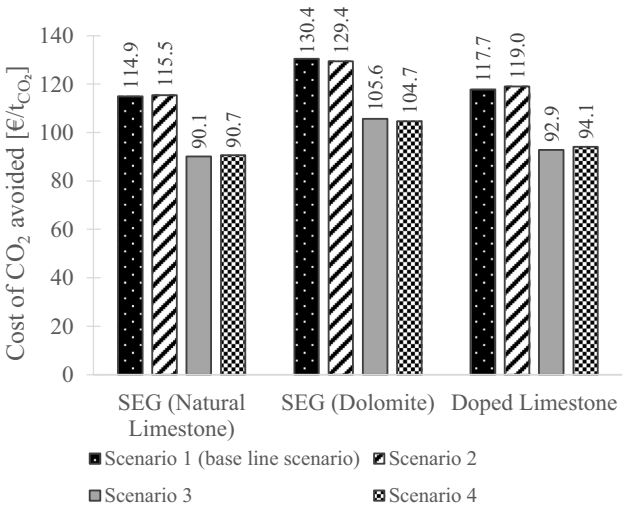

Fig. 5 Comparison of cost of CO_2 avoided for sorption-enhanced gasification using natural limestone, dolomite and doped limestone with seawater as sorbent, for the different scenarios

obtained in the case of doped limestone and thus, a higher H_2 production was achieved.

Regarding the baseline scenario (scenario 1) the *LCOH* increased from 2.7 (conventional gasification) to 5.4 or 5.0 €/kg of SEG using dolomite or SEG using doped limestone, respectively. These figures corresponded to a CO_2 avoided cost of 130.4 and 117.7 €/tCO_2 in the case of dolomite and doped limestone, respectively.

The application of a gate fee (scenario 2) decreased the *LCOH* of conventional gasification and SEG due to an additional revenue obtained by the waste management plant. While this reduction was more pronounced for conventional gasification, about 20.5%, in the case of SEG was about half of this figure for both sorbents, around 10.5%. Because both technologies benefited from this additional revenue, this difference was not reproduced on the cost of CO_2 avoided (Fig. 5), which varied just about 1%.

On the other hand, in scenario 3, as more than 90.0% of the CO_2 emissions were captured in the case of SEG, the levy of fossil CO_2 emissions reduced the cost of CO_2 avoided by around 20.0% (from 130.4 to 105.6 €/tCO_2, in the case of dolomite and 177.7 to 92.9 €/tCO_2, in the case of doped limestone) compared to baseline scenario 1. While the *LCOH* increased by 20.0% in the conventional gasification, the *LCOH* of SEG just increased by 0.6 and 0.8% in the case of dolomite and doped limestone, respectively (Fig. 4).

It can be observed in Fig. 4 that the application of both gate fee and fossil CO_2 emissions tax (scenario 4) did not impact the *LCOH* of conventional gasification. This happened because the additional revenue obtained from the gate fee compensated the additional cost regarding the tax on fossil CO_2 emissions. Nevertheless, the *LCOH* of SEG was

reduced by 10.0% (from 5.4 and 5.0 €/kg to 4.8 and 4.5 €/kg, for dolomite and doped limestone, respectively). This corresponded to a decrease in the cost of CO_2 avoided of around 20.0% when compared with the baseline Scenario 1 (130.4 against 104.7 and 117.7 against 94.1 €/tCO_2, in the case of dolomite and doped limestone, respectively).

4.3 Sensitivity analysis

Since there is still some uncertainty associated with the economic assessment and in particular to the capital cost of SEG, which is very scarce, a sensitivity analysis on the main economic parameters was performed. The effect of these parameters on the cost of CO_2 avoided was investigated by varying their values by ± 25% for the baseline scenario 1 (Fig. 6). The conventional gasification and SEG capital requirements, in addition to the prices of CO_2 transport and storage, electricity and sorbent were the parameters considered in the sensitivity analysis.

As can be seen in Fig. 6, the results are quite similar for both sorbents, with the capital requirement playing the main role in the cost of CO_2 avoided. An increase of 25% in the capital cost of SEG led to a 43.3% and 45.6% increase in the cost of CO_2 avoided for dolomite and doped limestone, respectively. On the other hand, the cost of CO_2 avoided can be lowered by 26.3% and 30.3% for dolomite and doped limestone, respectively, if the capital required by conventional gasification rises by 25%. The only difference observed between the two sorbents stems from the difference in the sorbent cost. While the variation of ± 25% on dolomite price changed the cost of CO_2 avoided by no more than ± 0.8%, the cost associated with the doped dolomite can influence the cost of CO_2 avoided by ± 2.2%. This can be explained by the fact that it was assumed that the price of doped limestone (58.0 €/t) was 5 times the price of natural limestone (11.6 €/t), the latter was assumed to be the price of dolomite. For that reason, and since there is no precise cost associated with doping limestone, a further sensitivity for the baseline scenario (no gate fee or fossil CO_2 emissions tax) was carried out.

To understand how the cost of doped limestone influences the SEG MSW viability, the effect of the doped limestone price on the *LCOH* and the cost of CO_2 avoided was assessed. The price of the doped limestone was varied from

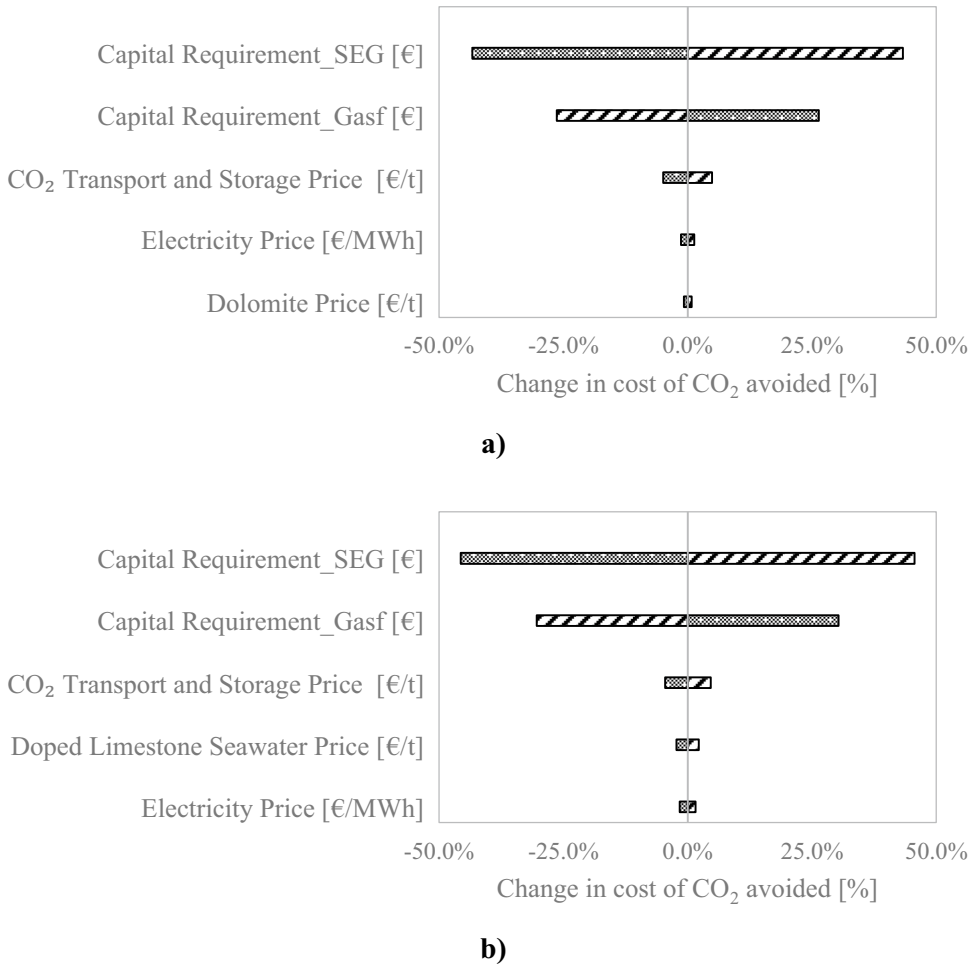

Fig. 6 Effect of the main economic parameters on the cost of CO_2 avoided: (**a**) using dolomite as sorbent and (**b**) using doped limestone with seawater as sorbent. Bubbles: − 25% of baseline parameter; stripes: + 25% of baseline parameter

11.6 €/kg (limestone price) to 116 €/kg (10× limestone price). The results are shown in Fig. 7. It can be observed that the *LCOH* can vary from 4.9 to 5.2 €/kg, which corresponds to a cost of CO_2 avoided between 109.3 and 128.4 €/tCO_2. Thus, if the doping process did not impose any cost penalty on sorbent price, the use of doped limestone would slightly reduce the *LCOH* from 5.0 (natural limestone) to 4.9 €/kg, followed by a reduction of 5% on the cost of CO_2 avoided.

The comparison of SEG performance using dolomite and doped limestone with that of SEG using natural limestone and conventional gasification is presented in Table 4. It should be mentioned that the optimum conditions for each case were a trade-off between H_2 productivity and net power efficiency. Thus, in all cases, it was considered an energetic self-sufficient plant.

Regarding the thermodynamic performance, the technology SEG using doped limestone presented a higher H_2 production efficiency, 50.0%. This can be attributed to the enhanced CO_2 sorption capacity of doped limestone. When compared with conventional gasification, this higher H_2 productivity was obtained at the expense of electrical power production. The net power efficiency of conventional gasification (6.0%) was more from 5 percentage points than that of SEG using doped limestone (0.6%).

As can be seen from Table 4, the integration of CO_2 capture, SEG, led to a reduction of more than 90% of equivalent CO_2 emissions. These decreased from 21.7 kg_{CO_2}/kg_{H_2}. (conventional gasification) to the range between 1.0 and 1.8 kg_{CO_2}/kg_{H_2}.

The economic assessment has shown that the introduction of CO_2 capture doubles the *LCOH* when dolomite was used as a sorbent. Between the natural and doped limestone, the former presented a lower cost of CO_2 avoided (114.9 €/tCO_2) than the latter (117.7 €/tCO_2). It is noteworthy that in the analysis of doped limestone, the energy penalty associated with sorbent drying was associated with the higher sorbent price. However, it is clear from Fig. 7 that if the cost of doped limestone is reduced to below 42.6 €/t, this sorbent would present the lowest cost of CO_2 avoided. Thus, the doped limestone seems to be a route that should be explored to replace natural limestone, whose one of the main drawbacks is the deactivation over the cycles.

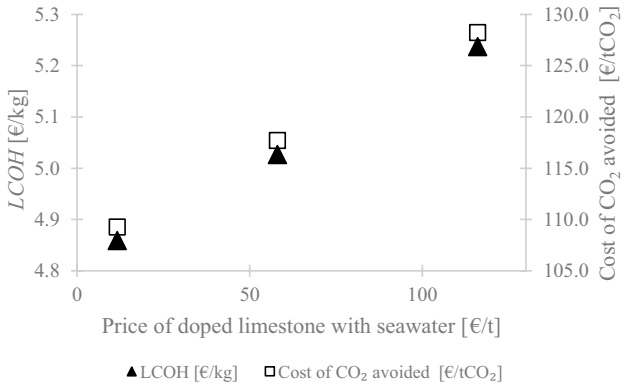

Fig. 7 Effect of doped limestone price on the levelised cost of hydrogen and cost of CO_2 avoided

5 Conclusions

In this work, the techno-economic performance of MSW SEG using three CaO-based sorbents, natural limestone, dolomite and doped limestone, was compared. While the H_2 production was one of the key thermodynamic performance indicators selected, the *LCOH* and cost of CO_2 avoided were the key economic performance indicators. The use of limestone as sorbent has shown to have the best techno-economic performance. The *LCOH* of SEG using dolomite is 5.4 €/kg against 5.0 €/kg when the limestone is used as sorbent. The natural limestone has shown to have the lowest cost of CO_2 avoided (114.9 €/tCO_2), whereas the doped limestone had the highest H_2 production efficiency (50.0%). In this work, the heat

Table 4 Summary of techno-economic performance of conventional gasification and sorption-enhanced gasification. The latter was carried out for three sorbents: limestone, dolomite and doped limestone with seawater

Parameter	Conventional gasification	Sorption-enhanced gasification		
		Natural limestone	Dolomite	Doped limestone
Thermodynamic assessment				
H_2 production efficiency (%)	47.7	48.7	46.0	50.0
Gross power efficiency (%)	18.9	17.0	16.2	18.3
Net power efficiency (%)	6.0	0.6	0.8	0.6
Total efficiency (%)	53.3	49.3	46.8	50.6
Environmental assessment				
Equivalent CO_2 emissions ($\mathbf{kg_{CO_2}kg_{H_2}}$)	21.7	1.4	1.0	1.8
Economic assessment				
Levelised cost of H_2 (€/kg)	2.7	5.0	5.4	5.0
Cost of CO_2 avoided (€/tCO_2)		114.9	130.4	117.7

requirement in the calciner falls between 4.6 GJ/tCO_2 (doped limestone) and 4.9 GJ/tCO_2 (dolomite). These results revealed a link between the heat requirement in the calciner and the H_2 production costs; however, detailed work on the effect of calcination temperature on energy requirement and overall costs should be carried out. A sensitivity analysis on the cost of CO_2 avoided was also performed by varying the main economic parameters by ± 25%. The capital requirement of conventional gasification and SEG, the CO_2 transport and storage price, the electricity and sorbent prices were the selected parameters in the sensitivity analysis. From these parameters, the capital requirement has the greatest influence on the CO_2 avoided cost, a reduction of 25% of SEG capital cost reduced the cost of CO_2 avoided by more than 40%. Although there is no data available for doped limestone price, it was found that a reduction on its price to below 42.6 €/t would reduce the cost of CO_2 avoided to a value lower than that for natural limestone. Furthermore, new sorbents for CO_2 capture and H_2 production would be an attractive alternative to natural limestone if produced with similar costs to that of natural limestone.

Nomenclature

a_1, a_2: fitting constant of sorbent maximum average conversion model (-); A_j: heat exchanger area of equipment j (m^2); *AC*: cost of CO_2 avoided (€/tCO_2); *ASU*: air separation unit; *b* : fitting constant of sorbent maximum average conversion model (-); *BFB*: bubbling fluidised bed; *CCS*: carbon capture and storage; *CEPCI*: Chemical Engineering Plant Cost Index; $e_{CO2,eq}$: equivalent CO_2 emissions ($kgCO_2/kgH_2$); *EUA*: CO_2 emission allowance price (€/tCO_2); f_1, f_2: fitting constant of sorbent maximum average conversion model (-); f_i: reaction extent (-); F_0 : fresh make-up sorbent rate (kmol/s); F_R : sorbent circulation rate (kmol/s); *LCOH*: levelised cost of hydrogen (€/kg); *LHV*: lower heating value (MJ/kg); $\dot{m}_i$: flowrate of component i (kg/s) or (t/h) or (kg/h); *MSW*: municipal solid waste; *NPV*: net present value (€); *PSA*: pressure swing adsorption; *SBR*: steam-to-biomass ratio (kg/kg); *SEG*: sorption-enhanced gasification; *TGA*: thermogravimetric analyser; $W_{el,\,gross}$: gross electric power output (MW_{el}); $W_{el,\,net}$: net electric power output (MW_{el}); $\dot{W}_j$: brake power requirement/output of equipment j (kW_{el})

Greek letters

η_{H_2}: H_2 production efficiency; $\eta_{el,\,gross}$: gross power efficiency; $\eta_{el,\,net}$: net power efficiency; $\eta_{el,\,net}$: total efficiency

Subscripts

ASU: air separation unit; *BRKP* : brake power; *calc*: calcination; *carb*: carbonation; *CCU* : CO_2 compression unit; *COND*: condensate; *CW* : freshwater; *DEA*: deaerator; *eq* : equivalent; *ECON*: economiser; *FC*: fuel compressor; *Gasf*: conventional gasification; *GT*: gas turbine; *HPST* : high-pressure steam turbine; *HPW* : high-pressure water; *HRSG* : heat recovery steam generator; *IPST* : intermediate-pressure steam turbine; *LPST* : low-pressure steam turbine; *LPW*: low-pressure water; *LS* : live steam

Supplementary Information The online version contains supplementary material available at https://doi.org/10.1007/s13399-022-02926-y.

Acknowledgements This publication is based on research conducted within the "Clean heat, power and hydrogen from biomass and waste" project funded by UK Engineering and Physical Sciences Research Council (EPSRC reference: EP/R513027/1).

Author contribution Monica P. S. Santos: conceptualization, methodology, investigation, formal analysis, visualisation, writing—original draft; Dawid P. Hanak: conceptualization, resources, data curation, writing—review and editing, supervision, project administration, funding acquisition.

Declarations

Conflict of interest The authors declare no competing interests.

Open Access This article is licensed under a Creative Commons Attribution 4.0 International License, which permits use, sharing, adaptation, distribution and reproduction in any medium or format, as long as you give appropriate credit to the original author(s) and the source, provide a link to the Creative Commons licence, and indicate if changes were made. The images or other third party material in this article are included in the article's Creative Commons licence, unless indicated otherwise in a credit line to the material. If material is not included in the article's Creative Commons licence and your intended use is not permitted by statutory regulation or exceeds the permitted use, you will need to obtain permission directly from the copyright holder. To view a copy of this licence, visit http://creativecommons.org/licenses/by/4.0/.

References

1. Statista (2021) Global historical CO_2 emissions from fossil fuels and industry 1750-2020. https://www.statista.com/statistics/264699/worldwide-c$_{o2}$-emissions/. Accessed 27 Oct 2021
2. IEA (2021) Global energy-related CO_2 emissions, 1990-2021, IEA, Paris. https://www.iea.org/data-and-statistics/charts/global-energy-related-co2-emissions-1990-2021. Accessed 27 Oct 2021
3. Intergovernamental Panel on Climate Change (2021) Summary for Policymakers. Climate Change 2021: ThePhysical Science Basis. Contribution of Working Group I to the Sixth Assessment Report of the Intergovernmental Panel on Climate Change
4. Yan J, Sun R, Shen L et al (2020) Hydrogen-rich syngas production with tar elimination via biomass chemical looping gasification (BCLG) using $BaFe_2O_4/Al_2O_3$ as oxygen carrier. Chem Eng J 387:124107. https://doi.org/10.1016/j.cej.2020.124107
5. Chen S, Zhao Z, Soomro A et al (2020) Hydrogen-rich syngas production via sorption-enhanced steam gasification of sewage sludge. Biomass and Bioenergy 138:105607. https://doi.org/10.1016/j.biombioe.2020.105607
6. Yang X, Tian S, Kan T et al (2019) Sorption-enhanced thermochemical conversion of sewage sludge to syngas with intensified

carbon utilization. Appl Energy 254:113663. https://doi.org/10.1016/j.apenergy.2019.113663
7. Marcantonio V, De Falco M, Capocelli M et al (2019) Process analysis of hydrogen production from biomass gasification in fluidized bed reactor with different separation systems. International Journal of Hydrogen Energy 44:10350–10360. https://doi.org/10.1016/j.ijhydene.2019.02.121
8. Schweitzer D, Albrecht FG, Schmid M et al (2018) Process simulation and techno-economic assessment of SER steam gasification for hydrogen production. International Journal of Hydrogen Energy 43:569–579. https://doi.org/10.1016/j.ijhydene.2017.11.001
9. Li W, Li Q, Chen R et al (2014) Investigation of hydrogen production using wood pellets gasification with steam at high temperature over 800 °C to 1435 °C. International Journal of Hydrogen Energy 39:5580–5588. https://doi.org/10.1016/j.ijhydene.2014.01.102
10. Hussain M, Zabiri H, Uddin F et al (2021) Pilot-scale biomass gasification system for hydrogen production from palm kernel shell (part B): dynamic and control studies. Biomass Conversion and Biorefinery. https://doi.org/10.1007/s13399-021-01733-1
11. Lazzarotto IP, Ferreira SD, Junges J et al (2020) The role of CaO in the steam gasification of plastic wastes recovered from the municipal solid waste in a fluidized bed reactor. Process Safety and Environmental Protection 140:60–67. https://doi.org/10.1016/j.psep.2020.04.009
12. Raizada A, Yadav S, Tripathi M et al (2021) Food waste treatment using in situ gasification after pyrolysis to produce hydrogen-rich syngas. Biomass Conversion and Biorefinery. https://doi.org/10.1007/s13399-021-01857-4
13. Irfan M, Li A, Zhang L et al (2019) Production of hydrogen enriched syngas from municipal solid waste gasification with waste marble powder as a catalyst. International Journal of Hydrogen Energy 44:8051–8061. https://doi.org/10.1016/j.ijhydene.2019.02.048
14. Foster W, Azimov U, Gauthier-Maradei P et al (2021) Waste-to-energy conversion technologies in the UK: processes and barriers – a review. Renewable and Sustainable Energy Reviews 135:110226. https://doi.org/10.1016/j.rser.2020.110226
15. Kaza S, Yao LC, Bhada-Tata P, Van Woerden F (2018) What a waste 2.0 : a global snapshot of solid waste management to 2050. Urban Development;. Washington, DC. World Bank, Washington, DC
16. Laurent A, Bakas I, Clavreul J et al (2014) Review of LCA studies of solid waste management systems - Part I: Lessons learned and perspectives. Waste Management 34:573–588. https://doi.org/10.1016/j.wasman.2013.10.045
17. Mehrpooya M, Ghorbani A, Ali Moosavian SM, Amirhaeri Y (2022) Optimal design and economic analysis of a hybrid process of municipal solid waste plasma gasification, thermophotovoltaic power generation and hydrogen/liquid fuel production. Sustainable Energy Technologies and Assessments 49:101717. https://doi.org/10.1016/j.seta.2021.101717
18. Mazzoni L, Janajreh I (2017) Plasma gasification of municipal solid waste with variable content of plastic solid waste for enhanced energy recovery. International Journal of Hydrogen Energy 42:19446–19457. https://doi.org/10.1016/j.ijhydene.2017.06.069
19. Yaqub ZT, Oboirien BO, Akintola AT (2021) Process modeling of chemical looping combustion (CLC) of municipal solid waste. Journal of Material Cycles and Waste Management. https://doi.org/10.1007/s10163-021-01180-0
20. Janajreh I, Adeyemi I, Elagroudy S (2020) Gasification feasibility of polyethylene, polypropylene, polystyrene waste and their mixture: experimental studies and modeling. Sustainable Energy Technologies and Assessments 39:100684. https://doi.org/10.1016/j.seta.2020.100684
21. Zheng X, Ying Z, Wang B, Chen C (2018) Hydrogen and syngas production from municipal solid waste (MSW) gasification via reusing CO_2. Applied Thermal Engineering 144:242–247. https://doi.org/10.1016/j.applthermaleng.2018.08.058
22. Lv L, Zhang Z, Li H (2019) SNG-electricity cogeneration through MSW gasification integrated with a dual chemical looping process. Chemical Engineering and Processing - Process Intensification 145:107665. https://doi.org/10.1016/j.cep.2019.107665
23. He M, Xiao B, Liu S et al (2009) Hydrogen-rich gas from catalytic steam gasification of municipal solid waste (MSW): Influence of steam to MSW ratios and weight hourly space velocity on gas production and composition. International Journal of Hydrogen Energy 34:2174–2183. https://doi.org/10.1016/j.ijhydene.2008.11.115
24. Hu M, Guo D, Ma C et al (2015) Hydrogen-rich gas production by the gasification of wet MSW (municipal solid waste) coupled with carbon dioxide capture. Energy 90:857–863. https://doi.org/10.1016/j.energy.2015.07.122
25. Zhou C, Stuermer T, Gunarathne R et al (2014) Effect of calcium oxide on high-temperature steam gasification of municipal solid waste. Fuel 122:36–46. https://doi.org/10.1016/j.fuel.2014.01.029
26. Martínez I, Grasa G, Callén MS et al (2020) Optimised production of tailored syngas from municipal solid waste (MSW) by sorption-enhanced gasification. Chemical Engineering Journal 401:126067. https://doi.org/10.1016/j.cej.2020.126067
27. Santos MPS, Hanak DP (2022) Techno-economic feasibility assessment of sorption enhanced gasification of municipal solid waste for hydrogen production. International Journal of Hydrogen Energy 47:6586–6604. https://doi.org/10.1016/j.ijhydene.2021.12.037
28. Rodríguez N, Alonso M, Abanades JC (2010) Average activity of CaO particles in a calcium looping system. Chemical Engineering Journal 156:388–394. https://doi.org/10.1016/j.cej.2009.10.055
29. Salaudeen SA, Acharya B, Dutta A (2018) CaO-based CO_2 sorbents: a review on screening, enhancement, cyclic stability, regeneration and kinetics modelling. Journal of CO_2 Utilization 23(179–199). https://doi.org/10.1016/j.jcou.2017.11.012
30. Chen J, Duan L, Sun Z (2020) Review on the development of sorbents for calcium looping. Energy & Fuels 34:7806–7836. https://doi.org/10.1021/acs.energyfuels.0c00682
31. Shokrollahi Yancheshmeh M, Radfarnia HR, Iliuta MC (2016) High temperature CO_2 sorbents and their application for hydrogen production by sorption enhanced steam reforming process. Chemical Engineering Journal 283:420–444. https://doi.org/10.1016/j.cej.2015.06.060
32. Zhang M, Peng Y, Sun Y et al (2013) Preparation of CaO-Al_2O_3 sorbent and CO_2 capture performance at high temperature. Fuel 111:636–642. https://doi.org/10.1016/j.fuel.2013.03.078
33. Radfarnia HR, Iliuta MC (2013) Metal oxide-stabilized calcium oxide CO_2 sorbent for multicycle operation. Chemical Engineering Journal 232:280–289. https://doi.org/10.1016/j.cej.2013.07.049
34. Zhao M, Bilton M, Brown AP et al (2014) Durability of CaO-$CaZrO_3$ sorbents for high-temperature CO_2 capture prepared by a wet chemical method. Energy and Fuels 28:1275–1283. https://doi.org/10.1021/ef4020845
35. Sun J, Guo Y, Yang Y et al (2019) Mode investigation of CO_2 sorption enhancement for titanium dioxide-decorated CaO-based pellets. Fuel 256:116009. https://doi.org/10.1016/j.fuel.2019.116009
36. Sedghkerdar MH, Mahinpey N, Sun Z, Kaliaguine S (2014) Novel synthetic sol-gel CaO based pellets using porous mesostructured silica in cyclic CO_2 capture process. Fuel 127:101–108. https://doi.org/10.1016/j.fuel.2013.08.007

37. Yin J, Zhang C, Qin C et al (2012) Reactivation of calcium-based sorbent by water hydration for CO_2 capture. Chemical Engineering Journal 198–199:38–44. https://doi.org/10.1016/j.cej.2012.05.078
38. Rong N, Wang Q, Fang M et al (2013) Steam hydration reactivation of cao-based sorbent in cyclic carbonation/calcination for CO_2 capture. Energy and Fuels 27:5332–5340. https://doi.org/10.1021/ef4007214
39. Sun J, Wang W, Yang Y et al (2020) Reactivation mode investigation of spent CaO-based sorbent subjected to CO_2 looping cycles or sulfation. Fuel 266:117056. https://doi.org/10.1016/j.fuel.2020.117056
40. Wu Y, Blamey J, Anthony EJ, Fennell PS (2010) Morphological changes of limestone sorbent particles during carbonation/calcination looping cycles in a thermogravimetric analyzer (TGA) and reactivation with steam. Energy and Fuels 24:2768–2776. https://doi.org/10.1021/ef9012449
41. Li Y, Zhao C, Chen H et al (2009) Modified CaO-based sorbent looping cycle for CO_2 mitigation. Fuel 88:697–704. https://doi.org/10.1016/j.fuel.2008.09.018
42. Salvador C, Lu D, Anthony EJ, Abanades JC (2003) Enhancement of CaO for CO_2 capture in an FBC environment. Chemical Engineering Journal 96:187–195. https://doi.org/10.1016/j.cej.2003.08.011
43. González B, Blamey J, Al-Jeboori MJ et al (2016) Additive effects of steam addition and HBr doping for CaO-based sorbents for CO_2 capture. Chemical Engineering and Processing: Process Intensification 103:21–26. https://doi.org/10.1016/j.cep.2015.09.019
44. Xu Y, Luo C, Zheng Y et al (2017) Natural calcium-based sorbents doped with sea salt for cyclic CO_2 capture. Chemical Engineering and Technology 40:522–528. https://doi.org/10.1002/ceat.201500330
45. González B, Kokot-Blamey J, Fennell P (2020) Enhancement of CaO-based sorbent for CO_2 capture through doping with seawater. Greenhouse Gases: Science and Technology 10:878–883. https://doi.org/10.1002/ghg.2013
46. Morona L, Erans M, Hanak DP (2019) Effect of seawater, aluminate cement, and alumina-rich spinel on pelletized CaO-based sorbents for calcium looping. Industrial & Engineering Chemistry Research 58:11910–11919. https://doi.org/10.1021/acs.iecr.9b00944
47. Armutlulu A, Naeem MA, Liu HJ et al (2017) Multishelled CaO microspheres stabilized by atomic layer deposition of Al_2O_3 for enhanced CO_2 capture performance. Advanced Materials 29:1–9. https://doi.org/10.1002/adma.201702896
48. De La Calle MA, Valverde JM, Sanchez-Jimenez PE et al (2016) Effect of dolomite decomposition under CO_2 on its multicycle CO_2 capture behaviour under calcium looping conditions. Physical Chemistry Chemical Physics 18:16325–16336. https://doi.org/10.1039/c6cp01149g
49. Fremaux S, Beheshti S-M, Ghassemi H, Shahsavan-Markadeh R (2015) An experimental study on hydrogen-rich gas production via steam gasification of biomass in a research-scale fluidized bed. Energy Conversion and Management 91:427–432. https://doi.org/10.1016/j.enconman.2014.12.048
50. Armbrust N, Duelli G, Dieter H, Scheffknecht G (2015) Calcium looping cycle for hydrogen production from biomass gasification syngas: experimental investigation at a 20 kW_{th} dual fluidized-bed facility. Industrial and Engineering Chemistry Research 54:5624–5634. https://doi.org/10.1021/acs.iecr.5b00070
51. Luz FC, Rocha MH, Lora EES et al (2015) Techno-economic analysis of municipal solid waste gasification for electricity generation in Brazil. Energy Conversion and Management 103:321–337. https://doi.org/10.1016/j.enconman.2015.06.074
52. Wang J, Cheng G, You Y et al (2012) Hydrogen-rich gas production by steam gasification of municipal solid waste (MSW) using NiO supported on modified dolomite. International Journal of Hydrogen Energy 37:6503–6510. https://doi.org/10.1016/j.ijhydene.2012.01.070
53. Zhen-Shan L, Ning-Sheng C, Li Z et al (2008) Process analysis of CO_2 capture from flue gas using carbonation/calcination cycles. AIChE Journal 54:1912–1925. https://doi.org/10.1002/aic
54. Romano MC (2013) Ultra-high CO_2 capture efficiency in CFB oxyfuel power plants by calcium looping process for CO_2 recovery from purification units vent gas. International Journal of Greenhouse Gas Control 18:57–67. https://doi.org/10.1016/j.ijggc.2013.07.002
55. Luberti M, Friedrich D, Brandani S, Ahn H (2014) Design of a H_2 PSA for cogeneration of ultrapure hydrogen and power at an advanced integrated gasification combined cycle with pre-combustion capture. Adsorption 20:511–524. https://doi.org/10.1007/s10450-013-9598-0
56. Hu M (2015) The new SeparALLTM process and PolybedTM PSA for IGCC and CTL application. In: 7th International Freiberg Conference Hohhot, China, June 7th-11th
57. Metz B, Davidson O, de Coninck H et al (2005) Carbon dioxide capture and storage. Cambridge University Press, Cambridge, New York; Melbourne; Madrid; Cape Town; Singapore; Sào Paulo
58. Santos MPS, Manovic V, Hanak DP (2021) Unlocking the potential of pulp and paper industry to achieve carbon-negative emissions via calcium looping retrofit. Journal of Cleaner Production 280:124431. https://doi.org/10.1016/j.jclepro.2020.124431
59. Hanak DP, Jenkins BG, Kruger T, Manovic V (2017) High-efficiency negative-carbon emission power generation from integrated solid-oxide fuel cell and calciner. Applied Energy 205:1189–1201. https://doi.org/10.1016/j.apenergy.2017.08.090
60. CEPCI (2020) The Chemical Engineering Plant Cost Index. In: Chemical Engineering. https://www.chemengonline.com. Accessed 5 Dec 2019
61. Bank of England (2019) Bank of England Statistical Interactive Database | Interest & Exchange Rates | Official Bank Rate History. http://www.bankofengland.co.uk/boeapps/iadb/repo.asp. Accessed 5 Dec 2019
62. Onarheim K, Santos S, Kangas P, Hankalin V (2017) Performance and cost of CCS in the pulp and paper industry part 2: economic feasibility of amine-based post-combustion CO_2 capture. International Journal of Greenhouse Gas Control 66:60–75. https://doi.org/10.1016/j.ijggc.2017.09.010
63. Maas W (n.d.) The post-2020 Cost-Competitiveness of CCS Cost of Storage
64. Martínez A, Lara Y, Lisbona P, Romeo LM (2014) Operation of a mixing seal valve in calcium looping for CO_2 capture. Energy and Fuels 28:2059–2068. https://doi.org/10.1021/ef402487e
65. Yang Y, Zhai R, Duan L et al (2010) Integration and evaluation of a power plant with a CaO-based CO_2 capture system. International Journal of Greenhouse Gas Control 4:603–612. https://doi.org/10.1016/j.ijggc.2010.01.004
66. Ember (2022) Daily Carbon Prices. https://ember-climate.org/data/carbon-price-viewer/. Accessed 24 Mar 2022
67. Haaf M, Ohlemüller P, Ströhle J, Epple B (2020) Techno-economic assessment of alternative fuels in second-generation carbon capture and storage processes. Mitigation and Adaptation Strategies for Global Change 25:149–164. https://doi.org/10.1007/s11027-019-09850-z
68. Ortiz C, Valverde JM, Chacartegui R (2016) Energy consumption for CO_2 capture by means of the calcium looping process: a comparative analysis using limestone, dolomite, and steel slag. Energy Technology 4:1317–1327. https://doi.org/10.1002/ente.201600390
69. Michalski S, Hanak DP, Manovic V (2019) Techno-economic feasibility assessment of calcium looping combustion using commercial

technology appraisal tools. Journal of Cleaner Production 219:540–551. https://doi.org/10.1016/j.jclepro.2019.02.049
70. Atsonios K, Koumanakos A, Panopoulos KD, et al (2013) Techno-economic comparison of CO_2 capture technologies employed with natural gas derived GTCC. In: Proceedings of the ASME Turbo Expo. p V002T07A018. https://doi.org/10.1115/GT2013-95117
71. Spallina V, Pandolfo D, Battistella A et al (2016) Techno-economic assessment of membrane assisted fluidized bed reactors for pure H_2 production with CO_2 capture. Energy Conversion and Management 120:257–273. https://doi.org/10.1016/j.enconman.2016.04.073
72. Kreutz T, Williams R, Consonni S, Chiesa P (2005) Co-production of hydrogen, electricity and CO from coal with commercially ready technology. Part B: Economic analysis. International Journal of Hydrogen Energy 30:769–784. https://doi.org/10.1016/j.ijhydene.2004.08.001
73. Lee YD, Ahn KY, Morosuk T, Tsatsaronis G (2014) Exergetic and exergoeconomic evaluation of a solid-oxide fuel-cell-based combined heat and power generation system. Energy Conversion and Management 85:154–164. https://doi.org/10.1016/j.enconman.2014.05.066
74. Shirazi A, Aminyavari M, Najafi B et al (2012) Thermal–economic–environmental analysis and multi-objective optimization of an internal-reforming solid oxide fuel cell–gas turbine hybrid system. International Journal of Hydrogen Energy 37:19111–19124. https://doi.org/10.1016/j.ijhydene.2012.09.143
75. Manzolini G, Macchi E, Gazzani M (2013) CO_2 capture in natural gas combined cycle with SEWGS. Part B: Economic assessment. International Journal of Greenhouse Gas Control 12:502–509. https://doi.org/10.1016/j.ijggc.2012.06.021
76. NREL (2005) Biomass to hydrogen production detailed design and economics utilizing the battelle columbus laboratory indirectly-heated gasifier. Technical Report NREL/TP-510-37408
77. Sayyaadi H, Mehrabipour R (2012) Efficiency enhancement of a gas turbine cycle using an optimized tubular recuperative heat exchanger. Energy 38:362–375. https://doi.org/10.1016/j.energy.2011.11.048
78. NETL (2019) Cost and performance baseline for fossil energy plants. Volume 1: Bituminous coal and natural gas to electricity. Technical Report NETL-PUB-22638

Publisher's note Springer Nature remains neutral with regard to jurisdictional claims in published maps and institutional affiliations.

https://dspace.org/

Sorption-enhanced gasification of municipal solid waste for hydrogen production: a comparative techno-economic analysis using limestone, dolomite and doped limestone

Santos, Mónica P. S.; Hanak, Dawid P.

2022-06-23
Springer
https://doi.org/10.1007/s13399-022-02926-y
Santos MP, Hanak DP. (2024) Sorption-enhanced gasification of municipal solid waste for hydrogen production: a comparative techno-economic analysis using limestone, dolomite and doped limestone, Biomass Conversion and Biorefinery, Volume 14, March 2024, pp. 7857-7872

Downloaded from a DSpace repository. https://dspace.org/